

Case Study

Improving Reliability of Protection Communication in a 5G Slice

Short title: Improving Protection Reliability in a 5G Slice

Petra Raussi ^{1*}, Heli Kokkonen-Tarkkanen ¹, Kimmo Ahola ¹, Antti Heikkinen ¹ and Mikko Uitto ¹

¹ VTT Technical Research Centre of Finland, Email: firstname.lastname@vtt.fi

*corresponding author: Tekniikantie 21, 02150 Espoo, Finland, Email: petra.raussi@vtt.fi

Author contributions: Petra Raussi: Conceptualization, Data curation, Formal analysis, Investigation, Methodology, Project administration, Resources, Software, Supervision, Validation, Visualization, Writing – original draft, Writing – review & editing Heli Kokkonen-Tarkkanen: Conceptualization, Data curation, Formal analysis, Funding acquisition, Investigation, Methodology, Project administration, Resources, Software, Validation, Visualization, Writing – original draft, Writing – review & editing Kimmo Ahola: Data curation, Methodology, Software, Writing – original draft, Writing – review & editing Antti Heikkinen: Data curation, Methodology, Software, Writing – original draft, Writing – review & editing Mikko Uitto: Data curation, Methodology, Software, Writing – original draft.

Funding: Business Finland, Grant/Award Numbers: 6392/31/2018 and 7263/31/2021.

Conflict of Interest statement: The authors declare no conflict of interest.

Permission to reproduce materials from other sources: None.

Data Availability statement: The data that support the findings of this study are available from the corresponding author upon reasonable request.

Abstract: 5G network slicing is a promising solution to prioritize time-critical protection communication in wireless networks. However, recent trends indicate that a 5G slice could encompass all smart grid applications lacking the necessary granularity. At the same time, while substation communication standards recommend prioritization of protection communication traffic to improve reliability, these recommendations are only for wired connections. Therefore, this paper investigates traffic shaping and uplink (UL) bitrate adaptation of video stream based on existing commercial solutions as methodologies for prioritizing the protection communication in a 5G slice. These methodologies are validated in an experimental setup combining controller-hardware-in-the-loop (CHIL) simulation with a quality of service (QoS) measurement system. The system under test consists of commercial 5G networks, commercial intelligent electronic devices (IEDs), and merging units to validate the methodologies on three smart grid applications: fault location, line differential, and intertrip protection. The results show improvement in protection communication when traffic shaping and UL bitrate adaptation are applied. Traffic shaping even improves prioritization with a wired connection.

Keywords: relay distribution grid automation, power system protection, reliability, electrical fault, 5G network, hardware-in-the-loop

1. Introduction

5G network slicing promises to provide tailored slices of the wireless communication channel for each vertical application, including the power system vertical. Mobile network operators have categorized the service portfolios based on three main use cases: ultra-reliable low-latency communication (URLLC), enhanced mobile broadband (eMMB), and massive machine type communication (mMTC). Each use case enables a different set of services to the end-user, such as a grid operator, who can select a use case and the corresponding services for their network slice. A combination of these use cases and associated services would be needed for smart grid substation communication to enable applications ranging from time-critical protection functions to video surveillance [1]. However, according to recent

industry developments, network slicing will lack the granularity required by power system utilities. The projected trend is that each company or vertical could purchase one network slice, which would be large enough to encompass all their operations [2]. Thus, utilities would have limited services enabled in their slice based on the selected use case. Depending on the selection, the slice's performance would be optimized to only a subset of the utility's applications. Meanwhile, other traffic within the slice makes critical protection communication more prone to delays and packet loss [3]. Therefore, further methodologies are needed inside the slice to ensure reliable substation communication.

Traditionally wired technologies have been used in power system communication due to the lack of reliability of the earliest generations of wireless technologies. A digital substation automation standard, International

Electrotechnical Committee (IEC) 61850 [4], gives detailed requirements for communication protocols at substations. IEC/TR 61850-90-4 [5], for example, emphasizes the importance of prioritization, separating critical data flows, and reducing unnecessary traffic by filtering, but the effects of all the recommended techniques do not persevere in wireless communication [5]. Without additional services, the user cannot affect traffic processing on a wireless network as the traffic leaves the local network.

Many methodologies for reliability and quality of service (QoS) preservation already exist and have been used for decades within wireless communication technologies but are currently re-emerging due to 5G URLLC latency and reliability requirements [6]. These methodologies include Hierarchical Token Bucket (HTB) queuing for traffic shaping based on traffic control at Linux kernel [7] to identify and rank the data packets according to their type and adapting the bitrate of uplink (UL) traffic of a live video stream. These methodologies have been selected for the investigation due to their availability and ease of implementation in existing commercial devices, accelerating the lab-to-market lead time. It might be also possible to achieve similar results by investing in separate hardware components, including routers, for each traffic flow, but this approach would increase the costs and is thus not considered in this paper. Based on the literature review, these methodologies have not been previously applied to smart grid substation communication traffic to prioritize mission-critical protection communication.

1.1. Related research

Previous literature on the usage of traffic shaping and HTB on Linux kernel is summarized in Table 1. Table 2 summarizes the testing and validation of protection applications by commercial intelligent electronic devices (IEDs) in commercial 5G networks. In the following, the related studies are examined, and the contributions of this paper are compared to the existing literature.

In [8], a traffic prioritization method using dynamic queuing with HTB is presented. Traffic prioritization is implemented for household routers. Therefore, similar prioritization, which is needed for distribution grid automation, is missing as all the customers are equal, and the prioritization is conducted based on the level of the data transfer rates compared to the traffic's time-criticalness. In [9], the main contribution is a cross-layer design for high-throughput data transfers. Three traffic shaping methods, Circuit TCP (CTCP), Token Bucket Filter (TBF), and HTB, are recommended for different use cases, and HTB in particular for multiple simultaneous large data transfers from a server. It is demonstrated that new HTB classes can be added without disrupting the existing traffic flows. The study overlooks a limited bandwidth in which it is not physically possible for all the traffic flows to be transmitted. In [10], an air time allocation algorithm is presented, which ensures fair air time allocation between high and low bandwidth users. This study focuses on WiFi, which uses an unlicensed spectrum, compared to 5G operating on a licensed spectrum. In [11], the optimization of high-priority agricultural machine communication via WiFi is presented using HTB. The dynamics of agricultural machines are slower than distribution grid communication causing significant difference in communication requirements. In [12], various QoS techniques, including HTB queuing at Linux routers, are

Table 1 Vertical applications for HTB traffic shaping in prior literature.

| Reference | Traffic shaping method | Vertical applications |
|-----------|------------------------|-------------------------|
| [6] | HTB | household router |
| [7] | HTB | transfers from a server |
| [8] | HTB | WiFi users |
| [9] | HTB | agricultural machines |
| [10] | HTB | MPEG video clips |

evaluated for three Moving Picture Experts Group (MPEG) video stream use cases. While video streaming is a part of the communication at digitalized substations, there is a lack of consideration for the rest of the traffic flows in a substation environment.

Linux traffic control has been previously implemented for smart grid use cases, but as a way to generate and shape generic wired communication channels to emulate various communication technologies such as 3G and 4G [13]. However, traffic control is not used to improve or prioritize the substation communication, only to generate desired communication channel. The heterogeneous nature of smart grid communication was realized decades ago, and traffic prioritization of smart grid communication has been presented for cognitive radio (CR) [14] and [15]. In [14] and [15], priority-based traffic scheduling and prioritized spectrum access scheme are suggested for CR communication. CR operates on the unlicensed spectrum, which can lack the reliability required for mission-critical protection communication compared to licensed 5G. The work is based on theoretical studies without realistic pilot environment validation with real smart grid communication data. Both [14] and [15] have unrealistically heterogeneous priority categories for the traffic flows, in which all substation automation communication is lumped into the highest priority category when there are diverse communication requirements within the category and substation communication itself. Similarly, [16] suggests CR secondary radio system as a suitable wireless technology for smart grid communication and provides a dynamic scheduling approach to account for the variable QoS priority of each device's data stream. However, the use case of smart meters requiring high QoS priority to report emergencies does not equal to the reliability requirements of protection communication. Both [17] and [18] propose scheduling algorithms for data transmission. In [17], the hierarchical adaptive weighting algorithm considers both delay and queue length improving the fairness of scheduling in the Long Term Evolution (LTE) network. The study overlooks protection and assigns the highest priority to a demand response control and the lowest priority to a remote substation control, which is not aligned with substation automation standards such as IEC 61850. The assumed delay budgets in the study are too long compared to utility recommendations [19]. In [18], priority based UL scheduling algorithm is developed to prioritize critical smart grid traffic in 5G URLLC. [18] presents a theoretical approach with assumption of each single cell in smart grid neighborhood area network idealistically containing one of each service type (distribution automation, video surveillance, charging

pile, distributed power supplies, Supervisory Control And Data Acquisition (SCADA), precise load control, and power failure detection) communication. Furthermore, both the approaches [17] and [18] are implemented as mathematical simulations rather than practical demonstration with real hardware and commercial networks lacking the input about the realistic capabilities of the wireless networks. In this paper, the focus is on sub-slice UL prioritization demonstrated in a commercial 5G non-standalone (NSA) network. In [8-12] HTB was used, but vertical use case was not smart grids. While in [14-18] vertical use case was smart grids, but the traffic shaping methods were prioritized spectrum access scheme, priority-based traffic scheduling, and hierarchical adaptive weighting algorithms.

Video streaming and cameras are used at digital substations for multiple purposes, including surveillance, thermal imaging, and image processing-based detection. For specific detection use cases, a high-definition video stream is required, which increases the video streaming data in the communication network, taking away an even larger share of the wireless communication bandwidth. If 5G network slicing is not offered at a highly granular level, the video stream must be transmitted via the same wireless communication channel as all other traffic at the substation, including protection communication. Another option would be to invest in a separate router for the video stream, but this would increase the costs, and both of the routers would still be connecting to the same base station via separate channels. In this paper, the focus is on a cost-optimized solution; therefore, the option with multiple routers is not considered. Instead, the aim is to limit the share of bandwidth of video streams, for which several methods are discussed in the following. Two decades ago, adjusting the bitrate of the output of the encoder at video monitoring of a substation was proposed [20]. However, the implementation is for a fiber channel, and two data types in the approach are video stream and alarms lacking the variety existing at digital substations. In [21], the video stream is operated event-based and triggered by Generic Object Oriented Substation Event (GOOSE) messages, but this method exposes GOOSE messages to unnecessary network sections, which might increase its vulnerability to cyber-attacks.

Typically the adaptation direction of a video stream is downlink (DL) occurring when consuming video content [22]. In contrast, at a substation, the adaptation is to UL direction since the camera generates the video stream, which is transferred to a control center. However, with the rise of content creation and live video streaming for entertainment purposes, few studies offer adaptation solutions for UL video streaming [23-25]. The use case of complex high-definition live streaming is the main focus, such as in [23] 360-video streaming. Due to the multiple video streams in 360-video, some duplicate footage can be discarded, and only video streams with suitable bitrate are combined into a 360-video [23]. In the substation environment, adjusting the bitrate by discarding recorded footage is not feasible, as cost optimization does not enable the installation of duplicate cameras. In [24], a video bitrate is dynamically adjusted to match the bandwidth by regulating quantization parameters. However, the study assumes fully utilizing the bandwidth of the LTE network. In this paper, the bitrate is adjusted at the encoder compared to the regulation of quantization parameters in a 5G network. In [25], an automatic video coding rate adjustment mechanism is used to adjust the video

Table 2 Testing using commercial 5G networks with real hardware IEDs for protection applications.

| Ref. | Hardware IEDs | Commercial communication network | 5G | Protection application |
|-------------------|---------------|----------------------------------|----|------------------------|
| [26-29] | - | - | - | - |
| [30-36] | - | - | - | ✓ |
| [37-39] | - | - | ✓ | ✓ |
| [40] | - | ✓ | ✓ | ✓ |
| [41-43] | ✓ | ✓ | - | - |
| [44-46] | ✓ | ✓ | - | ✓ |
| [47] | ✓ | - | - | - |
| [3, 48] | ✓ | - | - | ✓ |
| [49, 50] | - | ✓ | - | ✓ |
| [52, 53] | - | - | ✓ | - |
| this paper | ✓ | ✓ | ✓ | ✓ |

coding rate based on throughput in a Worldwide Interoperability for Microwave Access (WiMAX) channel. As outlined by [25], while the implementation is feasible, WiMAX lacks the overall bandwidth and low level of latency required by video streaming. The experiments are conducted in a generic urban environment without the information provided on the other data traffic types, compared to this paper in which the other traffic types are known and within the same vertical.

Due to the lack of recommendations for wireless technologies in smart grid communication, diverse implementations have taken precedence. Based on the development of wireless communications, the feasibility of various wireless technologies for smart grid communication has been researched over the years. An overview of the various studies compared to this paper is presented in Table 2. In [26-29], co-simulations of power systems and communication networks are conducted for capacitor bank, on-load tap changer (OLTC), and distributed generation control over WiMAX and LTE [26], for demand response control via Narrowband Internet of Things (NB-IoT) [27], and voltage control via LTE [28] and ZigBee [29]. In [30-36], co-simulation has been used to study various communication technologies such as CR [30], wireless local area network (WLAN) [31], customer 916.5 MHz channel [32], WiMAX [33, 36], wired [34, 35], and LTE [36] for protection applications, which include overcurrent protection [30, 34], fault detection [31], differential protection [32, 33, 35], adaptive protection [33], and disconnection of generation protection [36]. In [37-39], protection communication based on IEC 61850 Sampled Values (SV) and GOOSE over 5G has been studied with co-simulation. [39] studies usage of URLLC slice for teleprotection but assumes similar smart grid applications will be allocated to separate slices. [40] proposes a secure communication approach of routable GOOSE (R-GOOSE) messages via encapsulation or virtual private network (VPN), which is validated in a commercial 5G network by emulating R-GOOSE messages between Raspberry Pi and Linux PC lacking the realistic hardware IEDs. The validation is conducted using logic selectivity and

loss-of-mains protection applications [40]. In [41-43], hardware IEDs and commercial communication networks are used, but no protection applications nor 5G. In [41], NB-IoT is implemented for demand response control and [42] for a meter reading. In [43], WLAN is used for monitoring leakage currents. [44-46] study protection applications using hardware IEDs and commercial communication networks that lack 5G. [44] studies fault location over ZigBee, while [45] adaptive and line differential protection and [46] adaptive current differential protection and fault location over LTE. In [47] a hardware prototype is studied for control of microgrids via Long Range (LoRa). In [3, 48] ABB RED670 IEDs are used as hardware to study GOOSE and SV communication over presumably wired connection. In [49, 50], WiFi communication network is used to study line differential and overcurrent protection based on field measurements, while hardware prototype for loss-of-mains protection over Global System for Mobile (GSM) is studied in [51]. In [52] applicability of 5G for state estimation is studied with co-simulation and in [53] fault inspection over 5G and unmanned aerial vehicle (UAV) is simulated.

Compared to this paper, [26-40, 49, 50, 52, 53] do not use hardware IEDs but rather simulation software [26-31, 34-36, 52], Rapid61850 software [37], simulation based on measurements from hardware grid [49], simulation on the real-time operating system [50], hardware prototype [32], and emulated IEDs [38, 40, 53]. [33, 39] only consider communication networks. In [3, 26-39, 47, 48, 52, 53], commercial communication networks are not used, while in this paper commercial 5G network with a business subscription is employed. In [3, 26-36, 41-50], 5G technology is not considered, but other wireless and wired technologies, including NB-IoT [27, 41, 42], LTE [26, 28, 36, 45, 46], ZigBee [29, 44], CR [30], WLAN [31, 43], customer 916.5 MHz channel [32], WiMAX [26, 33, 36], wired [3, 34, 35, 48], LoRa [47], and WiFi [49, 50]. In [26-29, 41-43, 47, 52, 53], protection applications are not used; instead, the applications include capacitor bank, OLTC, distributed generation control [26], demand response control [27, 41], voltage control [28, 29], meter reading [42], leakage currents monitoring [43], microgrid control [47], state estimation [52], and fault inspection [53].

1.2. Contributions and structure

Most prior research on protection over wireless technologies is based on varying degrees of simulation. However, none of the prior studies combine commercially available 5G networks with controller-hardware-in-the-loop (CHIL) to study line differential, intertrip protection, and fault location like this paper. As many of the studies rely on pure simulation of the 5G networks, the results do not accurately portray the situation in the field. Utilities and power system component manufacturers are making investment decisions based on this research on the profitability of 5G. Therefore, it is critical to provide evidence of the 5G potential for smart grids based on pilot environments and field implementations to capture the true accuracy of the technology. Additionally, the data from the field can be input into simulations, further improving the accuracy of simulation-based feasibility studies.

Based on the identified research gap, the contribution of this paper is the following:

- Implement for the first time HTB traffic shaping and UL adaptation of video stream on substation communication traffic flows.
- Validate the methodologies in a novel experimental setup with CHIL simulation and system under test (SuT) consisting of several commercial IEDs, merging units, sensors, and camera exchanging data over a commercial 5G network.
- Compare the results of applying traffic shaping and UL traffic adaptation with reference measurements over a wired connection and with a variable number of different substation traffic streams.
- Demonstrate that traffic shaping improves reliability of protection communication even when using a wired connection.

Based on these contributions, this paper answers the following research questions:

1. *How much does applying traffic shaping increase the amount of successfully protected faults in non-congested and congested network scenarios?*
2. *How network congestion impacts successfulness of traffic shaping?*
3. *How much does adapting the live video stream UL bitrate increase the amount of successfully protected faults?*

The nomenclature of the used variables is listed in Table 3. The paper consists of five sections. The remainder of this paper is organized as follows: Section II introduces the optimization problem of the traffic flows within a slice and elaborates on the implemented traffic shaping and UL bitrate adaptation of video stream. Section III describes the experimental setup for the validation of the methodologies. Section IV discusses the measurements and their results. Finally, Section V concludes the paper and provides suggestions for future work.

Table 3 Nomenclature.

| | |
|--------------|---|
| ABR | adaptive bitrate |
| API | application programming interface |
| B | capacity of bandwidth |
| CHIL | controller-hardware-in-the-loop |
| CR | cognitive radio |
| C_T | total unavailable bandwidth at moment T |
| CTCP | Circuit TCP |
| C_{UL} | UL capacity |
| DASH | Dynamic Adaptive Streaming over HTTP |
| DL | downlink |
| eMMB | Enhanced Mobile Broadband |
| f | amount of traffic per type |
| f_{source} | amount of traffic at source |
| GOOSE | Generic Object Oriented Substation Event |
| GSM | Global System for Mobile |
| HTB | Hierarchical Token Bucket |
| HTTP | Hypertext Transfer Protocol |
| IEC | International Electrotechnical Committee |

| | |
|-------------|---|
| IED | intelligent electronic device |
| IP | Internet Protocol |
| JSON | Javascript Object Notation |
| K | segment of bandwidth |
| K_P | pre-defined segment of bandwidth |
| LoRa | Long Range |
| LTE | Long Term Evolution |
| m | number of traffic flows |
| MAC | media access control |
| MIKES | National Metrology Institute of Finland |
| mMTC | massive Machine Type Communication |
| MPEG | Moving Picture Experts Group |
| MQTT | Message Queuing Telemetry Transport |
| NB-IoT | Narrowband Internet of Things |
| NSA | non-standalone |
| OLTC | on-load tap changer |
| PTP | Precise Time Profile |
| QoS | quality of service |
| R_C | current bitrate |
| R-GOOSE | routable GOOSE |
| R_{MAX} | maximum bitrate of video |
| R_{MIN} | minimum bitrate of video |
| R-SV | routable SV |
| R_T | target bitrate |
| RTMP | Real-Time Messaging Protocol |
| S | safety margin |
| SCADA | Supervisory Control And Data Acquisition |
| SDN | Software Defined Networking |
| s_{noise} | noise in channel |
| SuT | system under test |
| SV | Sampled Values |
| TBF | Token Bucket Filter |
| TCP | Transmission Control Protocol |
| T_{UL} | measured UL throughput |
| T'_{UL} | rate of change of UL throughput |
| UAV | unmanned aerial vehicle |
| UDP | User Datagram Protocol |
| UL | uplink |
| URLLC | ultra-reliable low-latency communication |
| VPN | virtual private network |
| WiMAX | Worldwide Interoperability for Microwave Access |
| WLAN | wireless local area network |
| x | priority weight |

2. Evaluated prioritization methodologies

The prioritization methodologies are needed to handle the situation with the limited bandwidth of the wireless channel. It is unrealistic to expect an indefinite bandwidth to be available for the utility; instead, the grid operator and the wireless communication network provider have agreed to a maximum bandwidth available. Therefore, the problem proposition is to optimize the traffic within the limited bandwidth, ensuring critical traffic, such as trip signals at the substation, have the highest priority. This optimization problem can be presented as follows:

$$B = x_1 f_1 + x_2 f_2 + \dots + x_n f_n \quad (1)$$

where $B = 1$ and $1 \geq x_1 \geq x_2 \geq \dots \geq x_n \geq 0$, in which B is the capacity of the bandwidth, x is the weight indicating the traffic's priority, and f is the traffic's amount per type. The aim is to allocate the most critical traffic type and the consecutive traffic types per the bandwidth availability. If there is no bandwidth available to transmit, especially the least prioritized traffic types, then this traffic is dropped and not transmitted to ensure the transmission of the most critical traffic types. In industrial use cases, the prioritization philosophy is very different from consumer use cases, where all data traffic streams are considered equally important, in which case optimization focus is fairness among the data streams [6]. If the bandwidth is used in K segments [54], the allocation can be expressed as:

$$B = \sum_{i=1}^n x_i f_i / K_i \quad (2)$$

On the other hand, individual traffic sources can include control elements to adjust the amount of traffic sent at the source. If it is assumed the total unavailable bandwidth C at the moment T is known, then the amount of traffic at the source can be defined as:

$$f_{source} = B - C_T \quad (3)$$

where $f_{source_{min}} \leq f_{source} \leq f_{source_{max}}$. The amount of traffic generated from an individual traffic source is limited by the maximum amount of traffic a traffic source can generate and the minimum amount of traffic required to transmit understandable data. Based on this formula, the amount of traffic generated by individual sources becomes inversely correlated to the amount of allocated bandwidth and existing traffic in the wireless channel

$$f_{source} \propto C_T^{-1}. \quad (4)$$

The control of individual traffic sources could be combined with the optimization of the overall bandwidth use when it is known that individual traffic sources can be controlled. In this paper, only the lowest priority traffic stream can be controlled. Therefore, by combining formulas (1) and (3) can be derived

$$B = x_1 f_1 + x_2 f_2 + \dots + x_n (B - C_T). \quad (5)$$

However, if granularity to the level of individual priority classes, which typically consist of one or more traffic flows with similar communication requirements, is assumed, the

wireless channel could be divided into predefined segments K_P as follows

$$y = \sum_{i=1}^n m_{1,i} K_{P,1} + \sum_{i=1}^n m_{2,i} K_{P,2} + \dots + \sum_{i=1}^n m_{N,i} K_{P,N} + s_{noise}. \quad (6)$$

where $\sum_{i=1}^n K_i \leq B$, m is the number of traffic flows, and s_{noise} the noise in the channel. The predefined segments K_P could include dedicated service portfolios; therefore, formula (6) could represent a highly granular network slicing scenario. With the network slices' extreme granularity, other prioritization might not be crucial, but decreasing granularity implies that each traffic flow would consist of highly variable communication requirements necessitating further prioritization by alternative solutions. To explore the methodologies presented by formula (5), prioritization of all the egress traffic at the wireless channel is examined via traffic shaping and adjusting the amount of traffic from an individual traffic source via UL traffic adaptation of a live video stream.

Traffic shaping prioritizes communication traffic, allowing a fair share of critical communication to the network compared to non-critical traffic. It is a technique for Software Defined Networking (SDN) [55] and SDN-sliced networks that focuses on QoS optimization and bandwidth management by identifying and ranking different types of traffic flows and defining a share of bandwidth for each of them. Other methods to control and prioritize traffic include bandwidth management and traffic policing. Application-based traffic policing was selected over the other methods due to its practicality and suitability when dealing with critical communication traffic. It is applied at the output of a switching device according to the identified applications and traffic streams and their ranking based on requirements decided in advance. Compared to this, in bandwidth management, the traffic is typically controlled at a network link based on traffic measurements and the capacity of the link in order to avoid congestion in the link. While traffic policing can be implemented either at the input or output of a switching/routing device, its traffic contract to limit traffic output can cause high delays and even packet loss of critical communication if the source of the critical traffic is unaware of the traffic contract. Traffic shaping formats the traffic to the desired profile by delaying some or all packets and can be applied to improve QoS, optimize or guarantee performance, or expand usable bandwidth. Traffic shaping has been implemented in prior research on edge computing [56] and resource allocation [57].

Meanwhile, adjustment of individual traffic sources is conducted with live video stream adaptation, allowing a larger share of the bandwidth to be freed for critical communication, thus enabling fast recovery from network congestion. The adaptation system especially targets live video streaming as the operating environments of substations, and other remotely controlled units are increasingly monitored through video surveillance and sensors for faster reaction times, thereby reducing unnecessary high-cost physical intervention. In video adaptation, the main idea is to control which bitrate the video encoder can send data to the network or video player can receive data from the network. Usually, video adaptation is used when the UL or DL throughput varies, and the video application tries to match the

bitrate to the network capacity. One example of DL adaptation is Hypertext Transfer Protocol (HTTP) adaptive video streaming, such as Dynamic Adaptive Streaming over HTTP (DASH) [58], where the encoder or transcoder needs to create several versions of the same video at different bitrates. The videos are segmented into 1 to 10 s long segments, and the video player can select the most suitable version of the video based on the adaptive bitrate (ABR) algorithm. There are throughput-based, buffer-based, and hybrid ABR algorithms. In addition, the network-assisted adaptation can inform the video player of adaptation decisions when the ABR algorithm is, e.g., in the remote unit or the edge.

Another example is live video streaming, when the encoder sends video to UL to the video server or video player. If the network throughput varies or some other applications use the UL capacity, the end-to-end latency increases, and video quality suffers. A proactive video encoding service that adapts to network capacity based on 5G coverage is presented in [59].

2.1. Traffic shaping

Traffic shaping is implemented by Linux Traffic Controller [7] using HTB [60, 61]. HTB is formatted into classes, which can inherit tokens from the parent classes enabling flexible use of the available bandwidth [62]. The traffic is allowed to pass to the wireless channel when it is within a defined maximum rate. If the rate goes beyond the maximum, it will be either able to borrow tokens from the parent class or queued in a buffer, causing a delay in the data transmission. Traffic streams are assigned traffic types based on their Internet Protocol (IP) or media access control (MAC) address, associated with predefined priority and token amount. The operation of the HTB traffic shaping is depicted in Figure 1.

The traffic at the substation subject to traffic shaping consists of:

- IEC 61850-90-5 R-GOOSE and routable Sampled Values (R-SV) by two ABB RED615 IEDs,
- IEC 61850-9-2LE SV protocol in a VPN tunnel by two ABB SMU615 merging units and ABB SSC600 smart substation control and protection unit,
- Message Queuing Telemetry Transport (MQTT) protocol by Wirepass sensor network gateway sending periodic measures from several RUUVI sensors to the cloud server, and
- Transmission Control Protocol (TCP) protocol by Raspberry Pi streaming video in Real-Time Messaging Protocol (RTMP) format from Logitech Brio 4K Pro webcam to a cloud video server.

In addition, to study the network congestion scenario, there is additional User Datagram Protocol (UDP) traffic in the network. These traffic types are prioritized as per Table 4. The R-GOOSE and R-SV traffic is ranked the highest priority due to its nature as critical trip signals initiated by the protection application (R-GOOSE) and critical measurement data exchange required to keep the differential protection operational (R-SV). R-GOOSE and R-SV traffic accounts for 800 pps. SV traffic has the second highest priority, as fault indication is not as crucial as protection applications. SV traffic accounts for 4000 pps per device. The sensor and video traffic have consecutive priorities. Sensor traffic has higher priority due to its lesser amount, while video traffic is

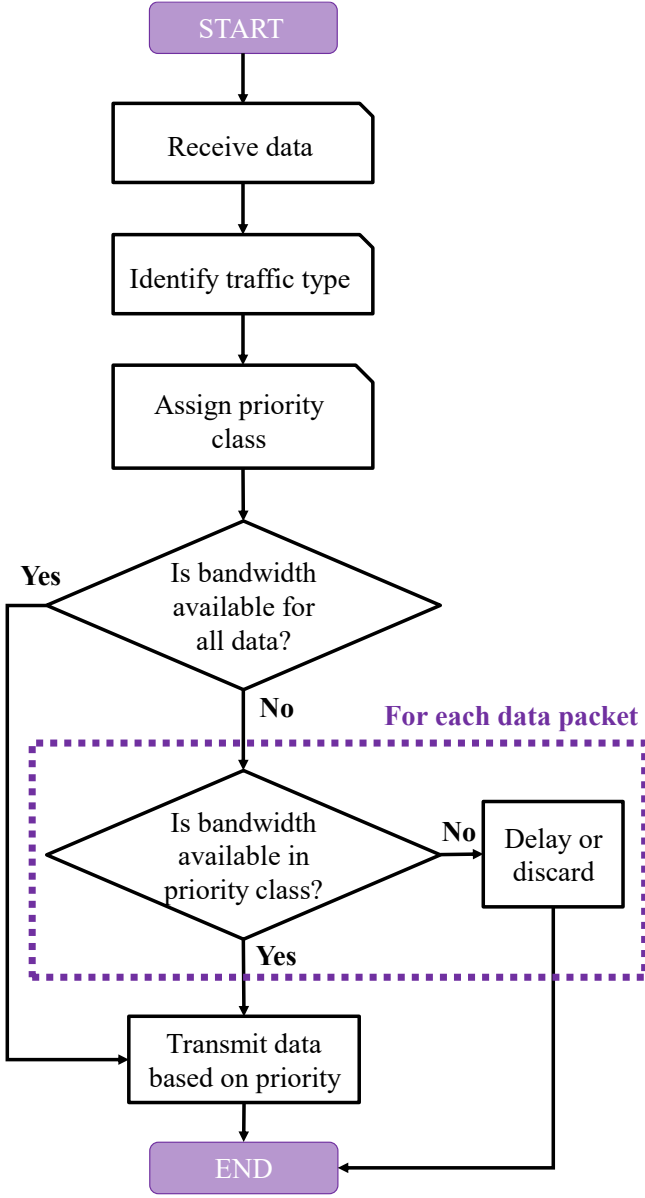


Figure 1 Traffic shaping operation flowchart

transmitted on best effort basis. If there is more data to be transmitted than the available bandwidth, then the data will be discarded or delayed. Discarding or delaying is started from the lowest priority class traffic, which is either additional UDP traffic or video traffic. The additional UDP traffic has the lowest priority and is only used to congest the network to assess the operation of the traffic shaping during network congestion.

Table 4 Traffic prioritization by traffic type.

| Traffic type | Avg. data transfer rate | Priority level |
|------------------------|-------------------------|----------------|
| R-GOOSE and R-SV | 1.3 Mbps | 1 |
| SV | 3.6-3.9 Mbps | 2 |
| sensor traffic | 500 Kbps | 3 |
| video traffic | 5 Mbps | 4 |
| additional UDP traffic | 10 Mbps | 5 |

Algorithm 1 Uplink bitrate adaptation of video stream

Input

C_{UL} : UL capacity
 R_{MAX} : maximum bitrate of video
 R_{MIN} : minimum bitrate of video
 T_{UL} : measured UL throughput
 T'_{UL} : rate of change of UL throughput
 $T'_{UL} > 0$ if T_{UL} increases
 $T'_{UL} < 0$ if T_{UL} decrease
 R_C : current bitrate
 S : safety margin (e.g., R_{MIN})

Output

R_T : target bitrate

```

1: procedure GET_TARGET_BITRATE
2:   /* Decrease target bitrate */
3:   if  $T'_{UL} > 0$  then
4:      $R_T = C_{UL} - T_{UL} - T'_{UL} * S$ 
5:   /* Increase target bitrate */
6:   else if  $T'_{UL} < 0$  then
7:      $R_T = R_C - T'_{UL} * S$ 
8:   else then
9:      $R_T = R_C$ 
10:  end if
11:  if  $R_T \geq R_{MAX}$  then
12:     $R_T = R_{MAX}$ 
13:  end if
14:  if  $R_T \leq R_{MIN}$  then
15:     $R_T = R_{MIN}$ 
16:  end if
17:  return  $R_T$ 
18: end procedure
  
```

2.2. Uplink bitrate adaptation of video stream

Adjusting UL traffic at the source is implemented as an adaptation system for the video stream bitrate the encoder sends to the control center from the substation. The adaptation algorithm adjusts the encoder target bitrate R_T based on the measured UL throughput T_{UL} . The initial value of the algorithm is the UL capacity C_{UL} , allocated to the use of the substation, and the maximum and minimum bitrates of the video R_{MAX} and R_{MIN} , respectively. Based on the measured UL throughput values, rate of change of the UL throughput T'_{UL} , and current bitrate R_C , the algorithm adjusts the new target bitrate between the minimum and maximum bitrates. Computing the new target bitrate includes a safety margin s , which is multiplied by the rate of change of UL throughput. Thus, when UL throughput increases and the rate of change is larger than zero, the target bitrate is decreased by a greater amount relative to the change. Vice versa, when the UL throughput decreases and the rate of change is smaller than zero, the target bitrate increases by a greater amount relative to the change. This adaptation algorithm is provided in Algorithm 1. The minimum bitrate is chosen to produce acceptable quality. If the video's bitrate is too low, it will be useless, so it is better to stop the encoder. The adaptation

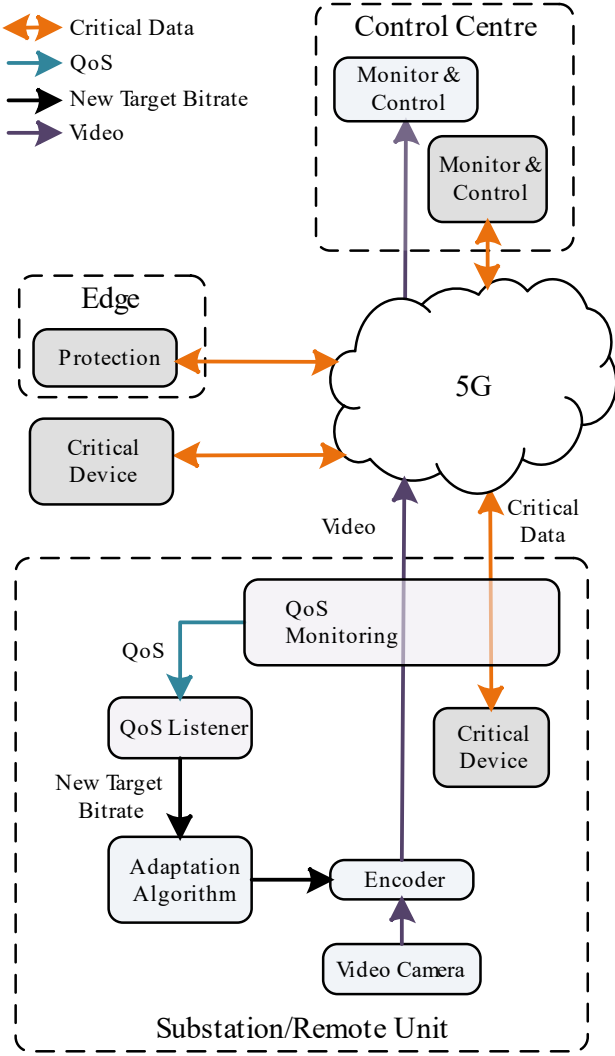


Figure 2 The video adaptation system at substation

algorithm component with the decision-making policy can also be placed flexibly in the network, for instance, on an edge separate from the encoder. Only the new target bitrate must be passed to the encoder in that case.

The adaptation system is depicted in Figure 2. The camera and the protection devices at the substation send UL live video stream and critical data, respectively. The critical data has a higher priority than the video. The system monitors the outgoing data from the substation and adapts the video bitrate to ensure the transfer of critical data. For this paper, a preliminary version of the video adaptation system is implemented where the main components are an encoder, a QoS monitoring based on the Qosium Probes and Listener, an adaptation algorithm, and control signaling. The video encoder has been modified so that the new target bitrate can be passed to it from outside during encoding without interrupting the encoding process. The encoder is based on FFmpeg and uses h.264 encoding. It runs on a Raspberry Pi 4 computer. The encoder captures video from Logitech Brio 4K Pro webcam, encodes, and transmits the live video in RTMP format over 5G to the video server. The bitrate (quality) of a video can be reduced to a certain point without becoming unusable in terms of quality. When the network UL traffic increases, the video's bitrate can be reduced to guarantee critical protection communication traffic transmission from

the relays and merging units without delay. Furthermore, when UL traffic decreases, the video bitrate increases. Hence, by adapting the video, the transfer of critical traffic to the UL can be guaranteed.

UL channel monitoring provides essential network information in real-time for the adaptation algorithm. The QoS Monitoring sends the data logs to the QoS Listener, a database for the measured data. Several essential parameters are monitored, such as throughput, delay, jitter, and packet loss. These are monitored both in UL and DL directions. As mentioned earlier, the initial adaptation logic relies on decisions based on UL throughput. Future work will utilize more complex adaptation algorithms based on a mixture of several monitored parameters.

A dedicated application programming interface (API) was implemented for interconnecting the QoS Listener with the adaptation algorithm and encoder using MQTT protocol with Javascript Object Notation (JSON) interchange format. The API retrieves the network parameters from the Listener and encapsulates the values into JSON syntax, which is then used as the MQTT payload and published to the MQTT broker. The initial timing for the process was set according to the used monitoring software, which recorded and transmitted the data every 1 second to the QoS Listener, which also processed the data accordingly towards MQTT publishment. After this, the data is available to be subscribed by the adaptation algorithm. Therefore, it is possible to achieve a fast reaction time for the encoder against rapid changes in the UL.

3. Test System

The experimental setup combining CHIL simulation of protection applications and communication measurement system was built to validate the traffic shaping and UL adaptation of video stream. The setup is shown in Figure 3. Similar CHIL experimental setups have been explored previously in combination with, for instance, Omnet [63], Click Modular router [3, 48], and NS3 simulator [28, 34]. However, many previous experimental setups have been implemented with simulated communication networks, which cannot capture the intricacies of commercial communication networks. The experimental setup used in this paper expands the setups in [45] and [35] with three major aspects. The experimental setup:

- 1) can be used to test several protection applications,
- 2) can run an unlimited number of recurring automated tests to obtain statistically significant results, and
- 3) incorporates a commercial 5G network with a business subscription.

The experimental setup was designed to record round-trip time within the CHIL simulation loop and simultaneously measure one-way communication network latency. A medium-voltage power line is modeled on an RTDS real-time simulator. The protection devices were located along the power line to form segments. ABB RED615 line differential protection and control relays and SMU615 merging units were the devices under test and the hardware counterparts for the IEDs in the real-time simulation. Current and voltage measurements were supplied to the hardware devices via Omicron CMS 356 amplifiers, and closed-loop CHIL was achieved by digital feedback signals indicating a successful operation of the protection applications. The power system part is coupled with the communication networks at Hitachi

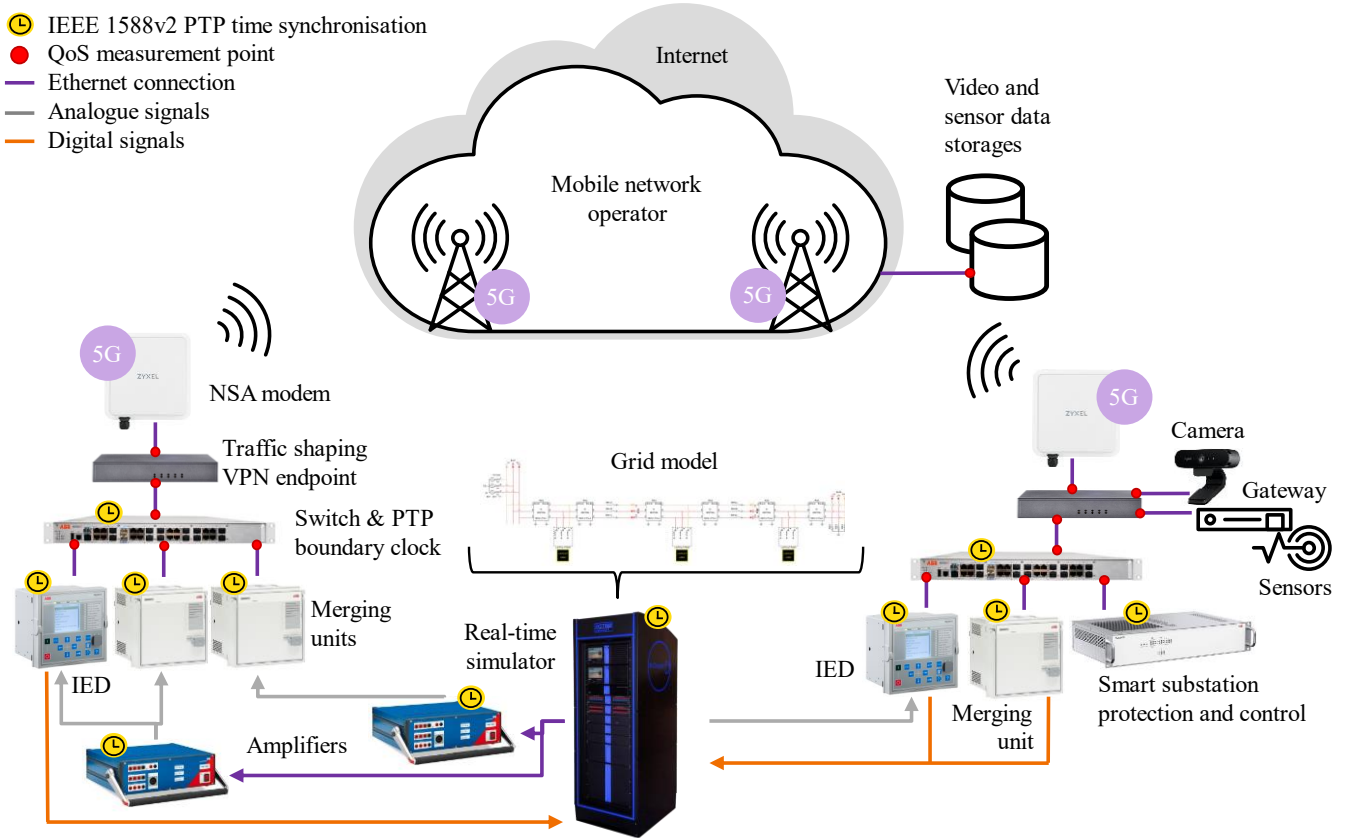


Figure 3 Overview of the experimental setup

Energy AFS677 network switches, through which data traffic is routed to the desired wireless network out of the available commercial and test 5G networks forming the SuT. The QoS measurement points at the network switches and VPN endpoints are indicated in Figure 3. The measurement points enable recording one-way latency for the end-to-end connection, including radio access and core network. The passive measurement system can record average and packet-level latency, jitter, and packet loss. The measurement system is based on Qosium, a passive measurement tool [64]. The measured traffic is mirrored to Qosium Probes, which send it forward to Qosium Scope and Listeners for real-time visualization. The results were simultaneously gathered with RSCAD Runtime, Qosium, and TCPDump tools and analyzed with Excel and MATLAB. All the equipment in the experimental setup was time-synchronized according to IEEE 1588v2 Precise Time Protocol (PTP) from the National Metrology Institute of Finland (MIKES) atomic clocks, enabling especially the accurate recording of one-way latencies. The video and sensor data traffic were generated to load the network in conjunction with other normal data traffic. The diverse selection of traffic was passed through the same wireless communication channel to illustrate a 5G slice

scenario in which the utility has only one slice for all operations.

In this paper, the traffic shaping and the UL traffic adaptation are validated with three applications: fault location, line differential, and intertrip protection, as shown in Figures 4 and 5. These applications were selected because of their strict and diverse communication requirements. In the fault location use case, a virtual fault passage indicator was implemented with directional overcurrent protection on an ABB SSC600 smart substation control and protection device

acting as an edge device. SSC600 indicates the fault location based on the SV streams from SMU615 merging units positioned along the feeder line. The SV streams are based on IEC 61850-9-2LE protocol, and as they are layer 2 traffic, a VPN connection is used to transmit the streams over a commercial 5G network. Wireless 5G was tested as a

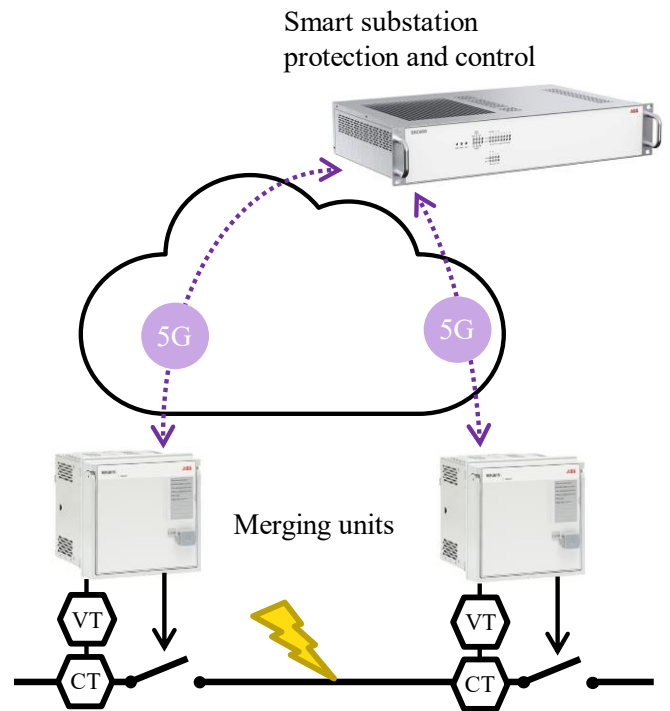


Figure 4 Diagram fault location use case

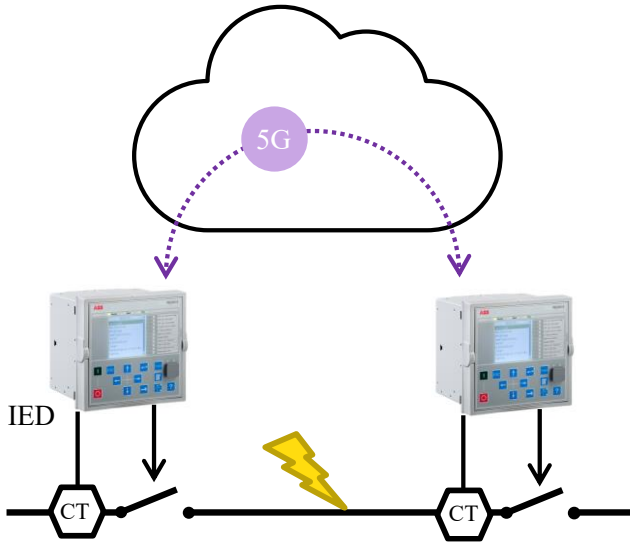


Figure 5 Diagram of line differential and intertrip protection use case

communication channel between the merging units and the edge device, as indicated in Figure 4.

Meanwhile, the line differential and intertrip protection use cases were implemented using RED615 relays, and wireless communication was applied to the data exchange of these relays, as depicted in Figure 5. These protection use cases are based on R-SV and R-GOOSE protocols. Line differential protection monitors differences in the current measurements of the two relays, initiates alarms in case of differences, and disconnects the entire line section between the relays in case of a fault. In intertrip protection, the local relay sends a trip command to a remote relay that is executed immediately. Intertrip protection is employed to protect transformers connected without circuit breakers or as breaker-failure protection.

4. Measurements and Results

The measurements were performed using the experimental setup with a commercial 5G NSA network. Reference measurements were conducted via a fixed Ethernet connection. Zyxel NR7101 industrial outdoor 5G routers were interconnected by fiber connections to the roof of the laboratory building at a distance of 400 meters from the base station and 130 m apart from one another. A common 'business' subscription was used on the commercial network, and the wireless routers were locked at 3500 MHz 5G cells with 2600 MHz and 1800 MHz cells as 4G anchors. Most of the traffic was routed to the first cell that was known to have a UL throughput-restrictive configuration. The traffic shaping and the UL bitrate adaptation were validated with QoS measurements of the R-GOOSE, R-SV, and SV data streams with various traffic combinations listed in Table 5. Results for the most critical R-GOOSE and R-SV streams are presented in Figures 6-8 and Tables 6-7. However, the overall results and conclusions contain a larger set of analyzed measurements.

For the critical traffic flows, latencies, jitters, packet losses, and connection breaks were measured. The critical traffic flows were mirrored to the Qosium measurement

Table 5 Cases for QoS measurements with and without traffic shaping (HTB).

| Case | 2x RED | 3x SMU | Sensor traffic | Video 5, 3, 1 Mb/s | Addit. 10 Mb/s | HTB |
|----------|-----------|-----------|-------------------|--------------------------|----------------------|-----|
| Case-1nr | ✓ | | | | | |
| Case-2nr | | ✓ | | | | |
| Case-3nr | ✓ | ✓ | | | | |
| Case-4nr | ✓ | ✓ | ✓ | | | |
| Case-5nr | ✓ | ✓ | ✓ | ✓ | | |
| Case-6nr | ✓ | ✓ | ✓ | ✓ | ✓ | |
| Case-1r | ✓ | | | | | ✓ |
| Case-2r | | ✓ | | | | ✓ |
| Case-3r | ✓ | ✓ | | | | ✓ |
| Case-4r | ✓ | ✓ | ✓ | | | ✓ |
| Case-5r | ✓ | ✓ | ✓ | ✓ | | ✓ |
| Case-6r | ✓ | ✓ | ✓ | ✓ | ✓ | ✓ |

probes at the network switches. Simultaneously with the QoS measurements, the CHIL setup was used to initiate overcurrent faults, monitor the overall operate times, and record the number of successfully protected faults. In addition, reference measurements were performed without traffic shaping and over a fixed connection to provide comparison case to the studied methodologies. All the other cases were measured twice, but cases 4nr (without traffic shaping) and 4r (with traffic shaping) were measured only once. Measurement times were 1-2 h per case, representing approximately a thousand generated faults per test.

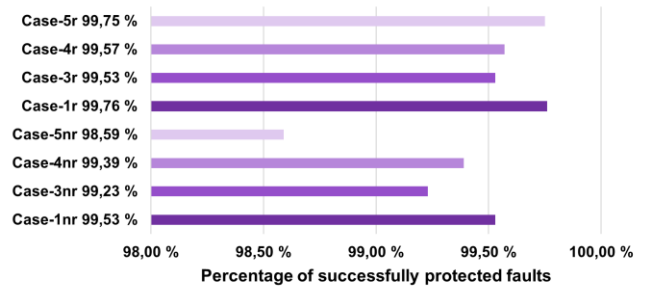


Figure 6 Communication traffic of 2xREDs, 3xSMUs, SSC, sensors, and additional traffic with (r) and without (nr) traffic shaping. Percentage of successfully protected faults

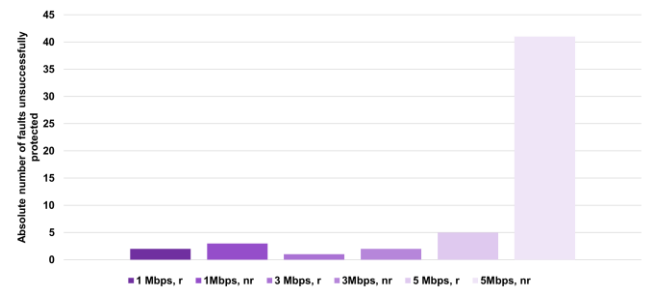


Figure 7 An absolute number of unsuccessfully protected faults with 5, 3, or 1 Mb/s of video traffic with (r) and without (nr) traffic shaping

Measurement results, presented in Figure 6, show an improvement in the number of successfully protected faults by an increase of 1.16 % (5nr vs. 5n) when the traffic shaping was applied. The results show the greatest improvement in the case of high video traffic in the communication channel. In the case with the most drastic improvement visible in Table 7, the total amount of traffic included R-GOOSE and R-SV communication from the IEDs, SV communication from merging units, sensor traffic, live video stream, and 10 Mb/s of additional traffic causing congestion in the wireless router. In this case (6nr and 6r) with congestion, the number of successfully protected faults increased from 51.84 % to 99.41 % with the traffic shaping.

The UL traffic adaptation limited the live video streaming traffic from 5 Mb/s to 3 Mb/s and 1 Mb/s and increased the number of successfully protected faults, as shown in Figure 7. This result is especially visible without traffic shaping. At 5 Mb/s of video streaming, only 96.12 % of faults were

successfully protected, while with 3 Mb/s and 1 Mb/s, the numbers of successfully protected faults were 99.81 % and 99.71 %, respectively. Figure 8 shows how the cumulative distribution functions of one-way latencies change between the cases. For comparison, the curves present non-congested (RED1-> RED2) and congested (RED2 -> RED1) communication directions on the left and the right, respectively.

The results of QoS measurements are presented in Table 6 for the normal conditions in the communication channel and Table 7 for a congested communication channel. The results naturally show that, in normal conditions, increasing traffic close to the 5G UL capacity deteriorates critical communication. However, the measurement results for the critical traffic streams with strict traffic shaping policies remain at the same level regardless of the amount of less critical traffic. Traffic shaping maintains the latency, jitter, and packet loss values well. Similarly, increased traffic

Table 6 QoS measurements for critical traffic in congestion cases with (r) and without (nr) traffic shaping. Note that the congestion tests were conducted on 04/2021 and the measurements presented in Table 7 on 09/2021; overall improvement in the performance of the commercial 5G NSA network can be seen in the results.

| Measurements without traffic shaping | Delay 1→2 [ms] | Delay 2→1 [ms] | Delay 1→2 (max)[ms] | Delay 2→1 (max)[ms] | Jitter 1→2 [ms] | Jitter 2→1 [ms] | Jitter 1→2 (max)[ms] | Jitter 2→1 (max)[ms] |
|--------------------------------------|----------------|----------------|---------------------|---------------------|-----------------|-----------------|----------------------|----------------------|
| Case-6nr | 24.813 | 37.887 | 39.800 | 91.504 | 1.923 | 1.785 | 13.915 | 41.535 |
| Case-6nr-5Mb/s | 24.864 | 59.843 | 39.762 | 179.670 | 1.926 | 1.910 | 13.842 | 85.253 |
| Case-6nr-3Mb/s | 24.798 | 29.492 | 39.686 | 60.293 | 1.917 | 1.728 | 13.767 | 26.574 |
| Case-6nr-1Mb/s | 24.815 | 26.695 | 39.988 | 44.733 | 1.927 | 1.730 | 14.168 | 17.869 |
| With traffic shaping | | | | | | | | |
| Case-6r | 24.505 | 26.182 | 39.302 | 42.628 | 1.921 | 1.735 | 13.802 | 17.022 |
| Case-6r-5Mb/s | 24.467 | 26.178 | 38.950 | 42.676 | 1.916 | 1.736 | 13.644 | 17.144 |
| Case-6r-3Mb/s | 24.512 | 26.150 | 39.321 | 42.598 | 1.917 | 1.734 | 13.703 | 17.056 |
| Case-6r-1Mb/s | 24.506 | 26.235 | 39.545 | 42.692 | 1.930 | 1.737 | 14.024 | 16.924 |

Table 7 QoS measurements for critical traffic in normal cases with (r) and without (nr) traffic shaping.

| Measurements without traffic shaping | Delay 1→2 [ms] | Delay 2→1 [ms] | Delay 1→2 (max)[ms] | Delay 2→1 (max)[ms] | Jitter 1→2 [ms] | Jitter 2→1 [ms] | Jitter 1→2 (max)[ms] | Jitter 2→1 (max)[ms] |
|--------------------------------------|----------------|----------------|---------------------|---------------------|-----------------|-----------------|----------------------|----------------------|
| Case-1nr | 20.697 | 22.659 | 33.097 | 35.766 | 1.920 | 1.886 | 11.851 | 10.611 |
| Case-3nr | 20.718 | 24.725 | 33.386 | 40.102 | 1.937 | 1.706 | 13.633 | 14.937 |
| Case-4nr | 20.764 | 24.938 | 33.140 | 40.607 | 1.937 | 1.708 | 13.374 | 15.228 |
| Case-5nr | 20.654 | 25.277 | 32.233 | 43.132 | 1.929 | 1.725 | 12.902 | 17.243 |
| Case-5nr-5Mb/s | 20.677 | 25.295 | 32.453 | 46.218 | 1.928 | 1.732 | 12.907 | 19.407 |
| Case-5nr-3Mb/s | 20.644 | 25.128 | 32.123 | 41.899 | 1.928 | 1.723 | 12.911 | 16.714 |
| Case-5nr-1Mb/s | 20.644 | 25.402 | 32.154 | 41.605 | 1.930 | 1.720 | 12.916 | 15.890 |
| With traffic shaping | | | | | | | | |
| Case-1r | 20.692 | 23.322 | 32.566 | 37.079 | 1.921 | 1.922 | 11.367 | 11.139 |
| Case-3r | 20.749 | 24.719 | 32.904 | 39.753 | 1.935 | 1.706 | 13.403 | 14.320 |
| Case-4r | 20.758 | 24.751 | 32.531 | 39.736 | 1.934 | 1.707 | 13.110 | 14.436 |
| Case-5r | 20.694 | 25.027 | 32.454 | 40.676 | 1.926 | 1.720 | 13.032 | 15.298 |
| Case-5r-5Mb/s | 20.775 | 25.017 | 32.612 | 40.960 | 1.928 | 1.723 | 13.120 | 15.671 |
| Case-5r-3Mb/s | 20.677 | 25.101 | 32.415 | 40.915 | 1.923 | 1.721 | 13.088 | 15.503 |
| Case-5r-1Mb/s | 20.648 | 24.980 | 32.358 | 40.249 | 1.926 | 1.716 | 12.901 | 14.847 |

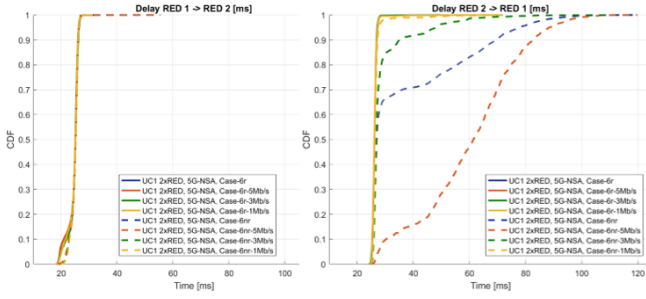


Figure 8 One-way latencies were measured for the critical traffic from RED1 to RED2 (on the left) and from RED2 to RED1 (on the right) with (r) and without (nr) traffic shaping. The router at the RED2 was congested to the UL direction using additional UDP traffic.

or congestion at the router did not cause a significant change in the percentage of successfully protected faults in the CHIL simulation.

When compared to [46], in which the delay was less than 80 ms and the system response time was within 200 ms for differential protection over a 4G LTE communication network, the results show that with a 5G NSA network, the average delays are within the range of 20 to 25 ms in the non-congested network, and the system operation times remain less than 30 ms. Occasional high latency peaks still exist, a typical phenomenon in wireless communication, but the maximum latencies are lower than in [46]. These results also align with the theoretical approach proposed in [18]. In addition, the experiments indicate that traffic shaping may even improve the performance of the wireless router, which is reflected in the results as lower maximum delays. However, verifying the results with much longer measurements would be good, increasing their statistical significance.

Despite the traffic shaping processing, an unexpected almost 200 us decrease in latency can be seen in most cases where the traffic shaping was used. The reference measurements also indicated that traffic shaping improves the overall QoS even when applied with a fixed connection. These results are aligned with [8], in which HTB-based traffic shaping was used in a completely different use case, household routers. The highest-priority users experienced a notable decrease in latency.

5. Conclusion

Smart grids are diverse communication environments having various communication requirements. 5G network slicing offers solutions for prioritizing mission-critical protection communication to a dedicated slice, but the recent trends show that network slicing could lack the required granularity to offer dedicated slices for each application. At the same time, smart grid substation automation standards, e.g., IEC 61850, lack recommendations on QoS preserving and prioritization techniques for wireless communication. Therefore, the prioritization of protection communication to increase its reliability in the 5G slice has been investigated with two methodologies from different perspectives. Traffic shaping looks at the prioritization of all traffic flows in the wireless network, while UL bitrate adaptation focuses on one traffic source, a live video stream, in the case of this paper. HTB traffic shaping and UL bitrate adaptation of video stream were successfully implemented for the first time

according to prior literature to prioritize protection communication among the substation communication traffic flows. Traffic shaping ranked the traffic by type and granted the highest priority to protection communication preserving its share transmitted to the network. The UL traffic adaptation adjusted the live video stream based on UL bitrate to enable a larger share of the bandwidth to be allocated for protection communication in case of high network load or congestion. These methodologies were validated in an experimental setup combining CHIL simulation with a QoS measurement system for wireless networks. Three applications of fault location, line differential, and intertrip protection were used for the validation operated on commercial IEDs and merging units interconnected with commercial 5G networks as the SuT. The substation communication traffic was based on IEC 61850 SV and GOOSE protocols and real data from sensors and video.

The results show that the parallel traffic flows deteriorate the QoS of protection communication. Based on the experiments, the research questions introduced can be answered as follows:

1. *How much does applying traffic shaping increase the amount of successfully protected faults in non-congested and congested network scenarios?* According to the results, the amount of successfully protected faults increased by 1.16 % in the non-congested scenario when traffic shaping was applied and by 47.57 % in the case of a congested network.
2. *How network congestion impacts successfulness of traffic shaping?* The results of the critical protection traffic remain at the same level with strict traffic shaping policies regardless of the amount of less critical traffic applied to congest the network. All parameters of latency, jitter, and packet loss remained at a good level.
3. *How much does adapting the UL bitrate of live video stream increase the amount of successfully protected faults?* The number of faults successfully protected was 96.12 % for 5 Mb/s of video streaming, 99.81 % for 3 Mb/s, and 99.71 % for 1 Mb/s. Therefore, the amount of successfully protected faults increased by 3.69 % by adapting the video traffic from 5 Mb/s to 3 Mb/s.

Based on the experiments, it seems clear that to maintain good QoS for critical applications, traffic shaping is crucial to be implemented in wireless routers (if supported) or in utility networking devices, especially in cases where a single wireless connection is used for various data flows. End-to-end network slicing should inherently maintain good QoS and priority for critical data flows. However, the experiments indicate that the slicing services should be considered per each application data flow to provide the best possible communication path for the most critical smart grid applications. In addition, the experiments show that adjusting the live video stream with the UL traffic adaptation also is a potential technique for self-healing to free up bandwidth if needed and thus enable fast recovery from network congestion. 5G network slicing is currently being implemented for commercial solutions. However, the solutions are still under development, allowing utilities to collaborate with manufacturers and telecommunication operators to ensure reasonable and functional slicing solutions for smart grids.

In the future, even longer duration measurements for traffic shaping and UL bitrate adaptation of video stream will

be conducted to expand the statistical results. UL bitrate adaptation will also be expanded to other traffic sources than video streams, and a more sophisticated adaptation algorithm based on several monitored parameters will be developed to adjust to various communication network conditions automatically.

6. Acknowledgments

This work was partly supported by the Finnish public funding agency for research, Business Finland, under the projects 5GVIIMA (6392/31/2018) and IFORGE (7263/31/2021). The projects are a part of the 5G Test Network Finland (5GTNF) ecosystem. The authors would also like to thank Sami Ruponen for his valuable support in solving hardware issues and Kalle Rauma for his valuable advice on journal writing that contributed to considerable improvements in this paper.

7. References

- [1] H. V. K. Mendis, P. E. Heegaard, V. Casares-Giner, F. Y. Li, and K. Kravetska, "Transient Performance Modelling of 5G Slicing with Mixed Numerologies for Smart Grid Traffic," in *2021 IEEE 26th International Workshop on Computer Aided Modeling and Design of Communication Links and Networks (CAMAD)*, 25-27 Oct. 2021, pp. 1-7, doi: 10.1109/CAMAD52502.2021.9617808.
- [2] I. Badmus, A. Laghrissi, M. Matinmikko-Blue, and A. Pouttu, "End-to-end network slice architecture and distribution across 5G micro-operator leveraging multi-domain and multi-tenancy," *EURASIP Journal on Wireless Communications and Networking*, vol. 2021, no. 1, p. 94, 2021/04/14 2021, doi: 10.1186/s13638-021-01959-7.
- [3] K. Pandakov, C. M. Adrah, H. K. Høidalen, and K. Ø. "Experimental Validation of a New Impedance-Based Protection for Networks With Distributed Generation Using Co-Simulation Test Platform," *IEEE Transactions on Power Delivery*, vol. 35, no. 3, pp. 1136-1145, 2020, doi: 10.1109/TPWRD.2019.2935834.
- [4] *Communication networks and systems for power utility automation*, I. 61850, 2022.
- [5] *Communication networks and systems for power utility automation*, I. T. 61850-90-4:2020, 2020.
- [6] N. Luangsomboon and J. Liebeherr, "HLS: A Packet Scheduler for Hierarchical Fairness," in *2021 IEEE 29th International Conference on Network Protocols (ICNP)*, 1-5 Nov. 2021, pp. 1-11, doi: 10.1109/ICNP52444.2021.9651972.
- [7] B. Hubert, "Linux Advanced Routing & Traffic Control HOWTO," <https://lartc.org/howto/> (accessed 2023).
- [8] T. Bakhshi and B. Ghita, "User-centric traffic optimization in residential software defined networks," in *2016 23rd International Conference on Telecommunications (ICT)*, 16-18 May 2016 2016, pp. 1-6, doi: 10.1109/ICT.2016.7500389.
- [9] F. Alali and M. Veeraraghavan, "A cross-layer design for large transfers in SDNs," in *2016 Eighth International Conference on Ubiquitous and Future Networks (ICUFN)*, 5-8 July 2016 2016, pp. 769-774, doi: 10.1109/ICUFN.2016.7537142.
- [10] Y. Fang, B. Doray, and O. Issa, "A Practical Air Time Control Strategy for Wi-Fi in Diverse Environment," in *2017 IEEE Wireless Communications and Networking Conference Workshops (WCNCW)*, 19-22 March 2017 2017, pp. 1-6, doi: 10.1109/WCNCW.2017.7919116.
- [11] M. Ruggeri, G. Malaguti, and M. Martelli, "Improvements of determinism in WI-FI real-time protocol for agricultural machine clusters," in *2012 IEEE International Symposium on Industrial Electronics*, 28-31 May 2012 2012, pp. 1846-1851, doi: 10.1109/ISIE.2012.6237373.
- [12] P. Shihyon and J. DeDorek, "Quality of service (QoS) for video transmission," in *2009 First International Conference on Ubiquitous and Future Networks*, 7-9 June 2009 2009, pp. 142-147, doi: 10.1109/ICUFN.2009.5174301.
- [13] C. Gavriluta, C. Boudinet, F. Kupzog, A. Gomez-Exposito, and R. Caire, "Cyber-physical framework for emulating distributed control systems in smart grids," *International Journal of Electrical Power & Energy Systems*, vol. 114, p. 105375, 2020/01/01/ 2020, doi: <https://doi.org/10.1016/j.ijepes.2019.06.033>.
- [14] J. Huang, H. Wang, Y. Qian, and C. Wang, "Priority-Based Traffic Scheduling and Utility Optimization for Cognitive Radio Communication Infrastructure-Based Smart Grid," *IEEE Transactions on Smart Grid*, vol. 4, no. 1, pp. 78-86, 2013, doi: 10.1109/TSG.2012.2227282.
- [15] R. Narayan Yadav, R. Misra, and S. Bhagat, "Spectrum access in cognitive smart-grid communication system with prioritized traffic," *Ad Hoc Networks*, vol. 65, pp. 38-54, 2017/10/01/ 2017, doi: <https://doi.org/10.1016/j.adhoc.2017.07.005>.
- [16] R. Yu, W. Zhong, S. Xie, Y. Zhang, and Y. Zhang, "QoS Differential Scheduling in Cognitive-Radio-Based Smart Grid Networks: An Adaptive Dynamic Programming Approach," *IEEE Transactions on Neural Networks and Learning Systems*, vol. 27, no. 2, pp. 435-443, 2016, doi: 10.1109/TNNLS.2015.2411673.
- [17] M. H. D. N. Hindia, F. Qamar, M. B. Majed, T. Abd Rahman, and I. S. Amiri, "Enabling remote-control for the power sub-stations over LTE-A networks," *Telecommunication Systems*, vol. 70, no. 1, pp. 37-53, 2019/01/01 2019, doi: 10.1007/s11235-018-0465-x.
- [18] L. Zhu, L. Feng, Z. Yang, W. Li, and Q. Ou, "Priority-Based uRLLC Uplink Resource Scheduling for Smart Grid Neighborhood Area Network," in *2019 IEEE International Conference on Energy Internet (ICEI)*, 27-31 May 2019 2019, pp. 510-515, doi: 10.1109/ICEI.2019.00096.
- [19] C. J. W. G. 34/35.11, "Protection using telecommunications," CIGRE, 2001. [Online]. Available: <https://e-cigre.org/publication/192-protection-using-telecommunications>
- [20] H. Huihui, C. Weirong, Q. Qingquan, and X. Liu, "Implementation of wide area communication in distributed remote video monitoring system for substations," in *The 2nd International Workshop on Autonomous Decentralized System*, 2002., 7-7 Nov. 2002 2002, pp. 294-298, doi: 10.1109/IWADS.2002.1194686.
- [21] Y. Su and X. Wang, "Video System Linkage Control with Relay Protection in Digital Substation," in *2010 Asia-Pacific Power and Energy Engineering Conference*, 28-31 March 2010 2010, pp. 1-4, doi: 10.1109/APPEEC.2010.5448448.
- [22] S. Wang, S. Bi, and Y. J. A. Zhang, "Deep Reinforcement Learning With Communication Transformer for Adaptive Live Streaming in Wireless Edge Networks," *IEEE Journal on Selected Areas in Communications*, vol. 40, no. 1, pp. 308-322, 2022, doi: 10.1109/JSAC.2021.3126062.
- [23] J. Li, R. Feng, W. Sun, Z. Liu, and Q. Li, "QoE-Driven Coupled Uplink and Downlink Rate Adaptation for 360-Degree Video Live Streaming," *IEEE Communications Letters*, vol. 24, no. 4, pp. 863-867, 2020, doi: 10.1109/LCOMM.2020.2966193.
- [24] P. Zhao, Y. Liu, J. Liu, R. Yao, S. Ci, and A. Argyriou, "Transmit power aware cross-layer optimization for LTE uplink video streaming," in *2015 IEEE International Conference on Communications (ICC)*, 8-12 June 2015 2015, pp. 6785-6790, doi: 10.1109/ICC.2015.7249407.
- [25] G. Ruiz, D. Pubill, F. Bader, and J. A. Ortega, "Video streaming in uplink mode using WiMAX system — experimental results," in *2009 IEEE 20th International Symposium on Personal, Indoor and Mobile Radio Communications*, 13-16 Sept. 2009 2009, pp. 598-602, doi: 10.1109/PIMRC.2009.5449786.
- [26] M. Ibrahim and M. M. A. Salama, "Smart distribution system volt/VAR control using distributed intelligence and wireless communication," *IET Generation, Transmission & Distribution*, vol. 9, no. 4, pp. 307-318, 2015, doi: <https://doi.org/10.1049/iet-gtd.2014.0513>.
- [27] Y. Li, X. Cheng, Y. Cao, D. Wang, and L. Yang, "Smart Choice for the Smart Grid: Narrowband Internet of Things (NB-IoT)," *IEEE Internet of Things Journal*, vol. 5, no. 3, pp. 1505-1515, 2018, doi: 10.1109/IIOT.2017.2781251.
- [28] F. Xie, C. McEntee, M. Zhang, B. Mather, and N. Lu, "Development of an Encoding Method on a Co-Simulation Platform for Mitigating the Impact of Unreliable Communication," *IEEE Transactions on Smart Grid*, vol. 12, no. 3, pp. 2496-2507, 2021, doi: 10.1109/TSG.2020.3039949.
- [29] M. You, X. Zhang, G. Zheng, J. Jiang, and H. Sun, "A Versatile Software Defined Smart Grid Testbed: Artificial Intelligence Enhanced Real-Time Co-Evaluation of ICT Systems and Power Systems," *IEEE Access*, vol. 8, pp. 88651-88663, 2020, doi: 10.1109/ACCESS.2020.2992906.

- [30] M. A. Hajahmed, M. Hawa, L. A. Shamlawi, S. Alnaser, Y. Alsmadi, and D. Abualnadi, "Cognitive Radio-Based Backup Protection Scheme for Smart Grid Applications," *IEEE Access*, vol. 8, pp. 71866-71879, 2020, doi: 10.1109/ACCESS.2020.2987762.
- [31] M. A. Zamani, A. Yazdani, and T. S. Sidhu, "A Communication-Assisted Protection Strategy for Inverter-Based Medium-Voltage Microgrids," *IEEE Transactions on Smart Grid*, vol. 3, no. 4, pp. 2088-2099, 2012, doi: 10.1109/TSG.2012.2211045.
- [32] D. R. Brown, J. A. Slater, and A. E. Emanuel, "A wireless differential protection system for air-core inductors," *IEEE Transactions on Power Delivery*, vol. 20, no. 2, pp. 579-587, 2005, doi: 10.1109/TPWRD.2005.844351.
- [33] T. S. Ustun and R. H. Khan, "Multiterminal Hybrid Protection of Microgrids Over Wireless Communications Network," *IEEE Transactions on Smart Grid*, vol. 6, no. 5, pp. 2493-2500, 2015, doi: 10.1109/TSG.2015.2406886.
- [34] T. Amare, C. M. Adrah, and B. E. Helvik, "A Method for Performability Study on Wide Area Communication Architectures for Smart Grid," in *2019 7th International Conference on Smart Grid (icSmartGrid)*, 9-11 Dec. 2019 2019, pp. 64-73, doi: 10.1109/icSmartGrid48354.2019.8990736.
- [35] M. Monadi, C. Koch-Ciobotaru, A. Luna, J. I. Candela, and P. Rodriguez, "Implementation of the differential protection for MVDC distribution systems using real-time simulation and hardware-in-the-loop," in *2015 IEEE Energy Conversion Congress and Exposition (ECCE)*, 20-24 Sept. 2015 2015, pp. 3380-3385, doi: 10.1109/ECCE.2015.7310137.
- [36] M. Garau, G. Celli, E. Ghiani, F. Pilo, and S. Corti, "Evaluation of Smart Grid Communication Technologies with a Co-Simulation Platform," *IEEE Wireless Communications*, vol. 24, no. 2, pp. 42-49, 2017, doi: 10.1109/MWC.2017.1600214.
- [37] V. G. Nguyen, K. J. Grinnemo, J. Cheng, J. Taheri, and A. Brunstrom, "On the Use of a Virtualized 5G Core for Time Critical Communication in Smart Grid," in *2020 8th IEEE International Conference on Mobile Cloud Computing, Services, and Engineering (MobileCloud)*, 3-6 Aug 2020 2020, pp. 1-8, doi: 10.1109/MobileCloud48802.2020.00009.
- [38] N. Kumari et al., "Enabling Process Bus Communication for Digital Substations Using 5G Wireless System," in *2019 IEEE 30th Annual International Symposium on Personal, Indoor and Mobile Radio Communications (PIMRC)*, 8-11 Sept. 2019 2019, pp. 1-7, doi: 10.1109/PIMRC.2019.8904287.
- [39] Z. Li et al., "Trade-off analysis between delay and throughput of RAN slicing for smart grid," *Computer Communications*, vol. 180, pp. 21-30, 2021/12/01/ 2021, doi: <https://doi.org/10.1016/j.comcom.2021.07.004>.
- [40] P. Jafary, A. Supponen, and S. Repo, "Network Architecture for IEC61850-90-5 Communication: Case Study of Evaluating R-GOOSE over 5G for Communication-Based Protection," *Energies*, vol. 15, no. 11, p. 3915, 2022. [Online]. Available: <https://www.mdpi.com/1996-1073/15/11/3915>.
- [41] A. K. Sultania, F. Mahfoudhi, and J. Famaey, "Real-Time Demand Response Using NB-IoT," *IEEE Internet of Things Journal*, vol. 7, no. 12, pp. 11863-11872, 2020, doi: 10.1109/JIOT.2020.3004390.
- [42] L. Wan, Z. Zhang, and J. Wang, "Demonstrability of Narrowband Internet of Things technology in advanced metering infrastructure," *EURASIP Journal on Wireless Communications and Networking*, vol. 2019, no. 1, p. 2, 2019/01/07 2019, doi: 10.1186/s13638-018-1323-y.
- [43] N. Harid, A. C. Bogias, H. Griffiths, S. Robson, and A. Haddad, "A Wireless System for Monitoring Leakage Current in Electrical Substation Equipment," *IEEE Access*, vol. 4, pp. 2965-2975, 2016, doi: 10.1109/ACCESS.2016.2577553.
- [44] J.-H. Teng, C.-H. Hsieh, S.-W. Luan, B.-R. Lan, and Y.-F. Li, "Systematic Effectiveness Assessment Methodology for Fault Current Indicators Deployed in Distribution Systems," *Energies*, vol. 11, no. 10, 2018, doi: 10.3390/en1102582.
- [45] P. Hovila et al., "5G networks enabling new smart grid protection solutions," in *25th International Conference on Electricity Distribution*, 2019: AIM - Association des Ingénieurs de Montefiore.
- [46] W. An, J. J. Ma, H. Y. Zhou, H. S. Chen, X. Jun, and X. Jian, "An Adaptive Differential Protection and Fast Auto-Closing System for 10 kV Distribution Networks Based on 4G LTE Wireless Communication," *Future Internet*, vol. 12, no. 1, p. 2, 2020. [Online]. Available: <https://www.mdpi.com/1999-5903/12/1/2>.
- [47] B. Arbab-Zavar, E. J. Palacios-Garcia, J. C. Vasquez, and J. M. Guerrero, "LoRa Enabled Smart Inverters for Microgrid Scenarios with Widespread Elements," *Electronics*, vol. 10, no. 21, p. 2680, 2021. [Online]. Available: <https://www.mdpi.com/2079-9292/10/21/2680>.
- [48] C. M. Adrah, K. Ø. Z. Liu, and H. K. Høidalen, "Communication network modeling for real-time HIL power system protection test bench," in *2017 IEEE PES PowerAfrica*, 27-30 June 2017 2017, pp. 295-300, doi: 10.1109/PowerAfrica.2017.7991240.
- [49] K. M. Abdel-Latif, M. M. Eissa, A. S. Ali, O. P. Malik, and M. E. Masoud, "Laboratory Investigation of Using Wi-Fi Protocol for Transmission Line Differential Protection," *IEEE Transactions on Power Delivery*, vol. 24, no. 3, pp. 1087-1094, 2009, doi: 10.1109/TPWRD.2009.2013665.
- [50] P. P. Parikh, T. S. Sidhu, and A. Shami, "A Comprehensive Investigation of Wireless LAN for IEC 61850-Based Smart Distribution Substation Applications," *IEEE Transactions on Industrial Informatics*, vol. 9, no. 3, pp. 1466-1476, 2013, doi: 10.1109/TII.2012.2223225.
- [51] M. Mekkanen and K. Kauhaniemi, "Wireless Light-Weight IEC 61850 Based Loss of Mains Protection for Smart Grid," *Open Engineering*, vol. 8, no. 1, pp. 182-192, 2018, doi: 10.1515/eng-2018-0022.
- [52] T. A. Zerihun, M. Garau, and B. E. Helvik, "Effect of Communication Failures on State Estimation of 5G-Enabled Smart Grid," *IEEE Access*, vol. 8, pp. 112642-112658, 2020, doi: 10.1109/ACCESS.2020.3002981.
- [53] Z. Ning, H. Chen, X. Wang, S. Wang, and L. Guo, "Blockchain-Enabled Electrical Fault Inspection and Secure Transmission in 5G Smart Grids," *IEEE Journal of Selected Topics in Signal Processing*, vol. 16, no. 1, pp. 82-96, 2022, doi: 10.1109/JSTSP.2021.3120872.
- [54] F. Baccelli and S. S. Kalamkar, "Bandwidth Allocation and Service Differentiation in D2D Wireless Networks," in *IEEE INFOCOM 2020 - IEEE Conference on Computer Communications*, 6-9 July 2020 2020, pp. 2116-2125, doi: 10.1109/INFOCOM41043.2020.9155469.
- [55] D. H. V. Tan, Q. Yang, K. Setlhapelo, O. Aggar, T. Godfrey, G. Stuebing, J. Mataboge, K. Li, V. Karantaev, H. Doi, M. Seewald, Z. Mbebe, L. Watts, M. Costa de Araujo, P. Zhang, C. Villasanti, G. Helps, S. Kacar, Z. Jiang, "Enabling software defined networking for electric power utilities," CIGRE, Technical Brochure, 2022, vol. 866.
- [56] P. Fondo-Ferreiro, D. Candal-Ventureira, F. Gil-Castiñeira, F. J. González-Castaño, and D. Collins, "Experimental Evaluation of End-to-end Flow Latency Reduction in Softwarized Cellular Networks through Dynamic Multi-Access Edge Computing," in *2021 IEEE 32nd Annual International Symposium on Personal, Indoor and Mobile Radio Communications (PIMRC)*, 13-16 Sept. 2021 2021, pp. 1310-1315, doi: 10.1109/PIMRC50174.2021.9569590.
- [57] M. Bosk et al., "Using 5G QoS Mechanisms to Achieve QoE-Aware Resource Allocation," in *2021 17th International Conference on Network and Service Management (CNSM)*, 25-29 Oct. 2021 2021, pp. 283-291, doi: 10.23919/CNSM52442.2021.9615557.
- [58] Information technology - dynamic adaptive streaming over HTTP (DASH), I. I. C. 23009-1:2014, 2014.
- [59] M. Uitto and A. Heikkinen, "Demo: Proactive Low Latency Video Encoding Service Based on 5G Coverage," in *2021 IEEE Vehicular Networking Conference (VNC)*, 10-12 Nov. 2021 2021, pp. 121-122, doi: 10.1109/VNC52810.2021.9644660.
- [60] Y. Benita, "Kernel korner: analysis of the HTB queuing discipline," *Linux Journal*, 01/01 2005.
- [61] D. G. Balan and D. A. Potorac, "Linux HTB queuing discipline implementations," in *2009 First International Conference on Networked Digital Technologies*, 28-31 July 2009 2009, pp. 122-126, doi: 10.1109/NDT.2009.5272182.
- [62] M. Devera, "Hierarchical token bucket theory," <http://luxik.cdi.cz/~devik/qos/htb/manual/theory.htm> (accessed).
- [63] K. Boroojeni, M. H. Amini, A. Nejadpak, T. Dragičević, S. S. Iyengar, and F. Blaabjerg, "A Novel Cloud-Based Platform for Implementation of Oblivious Power Routing for Clusters of Microgrids," *IEEE Access*, vol. 5, pp. 607-619, 2017, doi: 10.1109/ACCESS.2016.2646418.
- [64] Kaitotek, "Qosium," <https://www.kaitotek.com/qosium> (accessed 13.2.2023).

- [65] P. Hovila, H. Kokkonen-Tarkkanen, S. Horsmanheimo, P. Raussi, S. Borenius, and K. Ahola, "Cellular Networks providing Distribution Grid Communications Platform," in *26th International Conference on Electricity Distribution*, 2021.